

Study of the $h\gamma Z$ coupling at the ILC

Yumi Aoki¹, Keisuke Fujii², Sunghoon Jung³, Junghwan Lee³, Junping Tian⁴, Hiroshi Yokoya⁵
on behalf of the ILD concept group

SOKENDAI¹, KEK², Seoul National University³, University of Tokyo⁴,
KIAS⁵

February 19, 2020

Abstract

We study the $h\gamma Z$ coupling, which is a loop induced coupling in the Standard Model (SM), to probe new physics. In a global fit based on the SM Effective Field Theory, measurement of the SM $h\gamma Z$ coupling can provide a very useful constraint, in particular for the precise determination of hZZ and hWW couplings. At the International Linear Collider (ILC), there are two direct ways to study the $h\gamma Z$ coupling: one is to measure the branching ratio of the $h \rightarrow \gamma Z$ decay and the other to measure the cross section for the $e^+e^- \rightarrow h\gamma$ process. We have performed a full simulation study of the $e^+e^- \rightarrow h\gamma$ process at the 250 GeV ILC, assuming 2 ab^{-1} data collected by the International Large Detector (ILD). The expected 1σ bound on the effective $h\gamma Z$ coupling (ζ_{AZ}) combining measurements of the cross section for $e^+e^- \rightarrow h\gamma$ followed by $h \rightarrow b\bar{b}$ and the $h \rightarrow \gamma Z$ branching ratio is $-0.0015 < \zeta_{AZ} < 0.0015$. The expected significance for the signal cross section in the fully hadronic $h \rightarrow WW^*$ channel is 0.09σ for beam polarizations of $P(e^-, e^+) = (-80\%, +30\%)$.¹

1 Introduction

Precision study of the Higgs boson is a powerful tool to find physics beyond the standard model. The International Linear Collider (ILC) [1] is an ideal machine to carry out the precision Higgs measurements. Our motivation here is to probe new physics in $h\gamma\gamma$ and $h\gamma Z$ couplings. These two couplings in the Standard Model (SM) are both loop-induced therefore small new physics effects may show up as observable deviations from the SM. As one example, the expected deviations in the Inert Triplet Model [2] are shown in Fig. 1 for the $e^+e^- \rightarrow h\gamma$ cross section and the $h \rightarrow \gamma\gamma$ branching ratio, which suggests that, depending on model parameters, the deviations can be as large as 100%.

¹ Talk presented at the International Workshop on Future Linear Colliders (LCWS2019), Sendai, Japan, 28 October-1 November, 2019. C19-10-28.

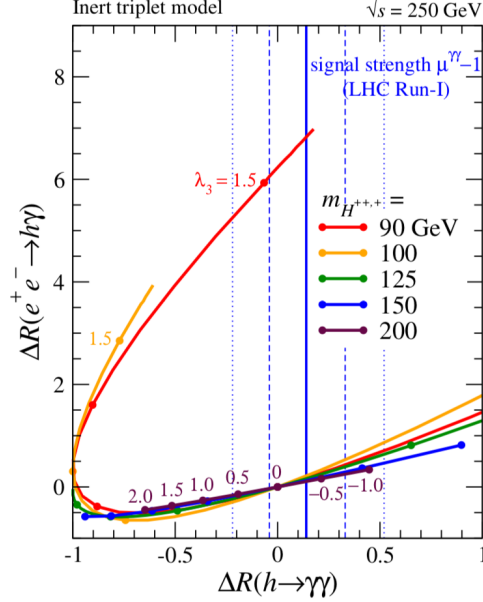


Figure 1: The relative deviations from the Standard Model for the $e^+e^- \rightarrow h\gamma$ cross section and the $h \rightarrow \gamma\gamma$ decay branching ratio [2].

A usual method to measure the $h\gamma\gamma$ and $h\gamma Z$ couplings is to use branching ratios of $h \rightarrow \gamma\gamma/\gamma Z$ decays. It is, however, challenging to measure the $h \rightarrow \gamma Z$ branching ratio: at the HL-LHC a 5σ significance is expected [3] and at the ILC only a significance of 2.3σ is expected [4]. As a complementary method we study these couplings in a production process at the ILC, $e^+e^- \rightarrow h\gamma$. A full simulation analysis in $h \rightarrow b\bar{b}$ channel has been reported in [14]. In this paper we focus on a new full simulation analysis of the fully hadronic $h \rightarrow WW^*$ channel.

This paper is organized as follows. In section 2, we explain how to measure $h\gamma Z$ coupling. Section 3 introduces our theoretical framework and experimental method. Our simulation framework is described in section 4. Section 5 gives the combined bound using the measurements of the $h \rightarrow \gamma Z$ branching ratio and the $e^+e^- \rightarrow h\gamma$ cross section. In section 6, we present a full simulation analysis for the fully hadronic $h \rightarrow WW^*$ channel. Finally, section 7 summarizes our results and concludes this paper.

2 Theoretical Framework and Experimental Method

We use the effective Lagrangian shown in Eq. 1 to include new physics contributions to the $e^+e^- \rightarrow h\gamma$ cross section in a model-independent way,

$$\mathcal{L}_{h\gamma} = \mathcal{L}_{\text{SM}} + \frac{\zeta_{AZ}}{v} A_{\mu\nu} Z^{\mu\nu} h + \frac{\zeta_A}{2v} A_{\mu\nu} A^{\mu\nu} h, \quad (1)$$

where, in addition to the first term from the SM, ζ_{AZ} and ζ_A terms represent, respectively, effective $h\gamma Z$ and $h\gamma\gamma$ couplings from new physics. $A_{\mu\nu}$ and $Z_{\mu\nu}$ are field strength tensors for the photon and the Z boson, respectively, and v is the vacuum expectation value.

The three terms contribute to the $e^+e^- \rightarrow h\gamma$ process via the Feynman diagrams shown in Fig. 2, where the first SM diagram represents several loop induced diagrams as shown in Fig. 3. The contributions from individual diagrams of Fig. 3 for unpolarized beams is shown Fig. 4. We can clearly see that there are significant destructive interferences between these diagrams. The SM cross sections at $\sqrt{s} = 250$ GeV are shown in Table 1, which are much less than 1 fb, indicating that experimental measurements would be challenging. The cross sections including effective $h\gamma Z/h\gamma\gamma$ couplings from new physics, normalized to their SM values, are given in Eq. 2 for beam polarizations $P(e^-, e^+) = (-100\%, +100\%)$ and in Eq. 3 for $P(e^-, e^+) = (+100\%, -100\%)$, up to interference terms.

$$\frac{\sigma_{\gamma H}}{\sigma_{SM}} = 1 - 201\zeta_A - 273\zeta_{AZ} \quad (2)$$

$$\frac{\sigma_{\gamma H}}{\sigma_{SM}} = 1 + 492\zeta_A - 311\zeta_{AZ} \quad (3)$$

Since ζ_A can be constrained by the measurement of the $h \rightarrow \gamma\gamma$ branching ratio at the (HL-)LHC, we can extract ζ_{AZ} by measuring the cross section of $e^+e^- \rightarrow h\gamma$ at the ILC for just one set of beams polarizations.

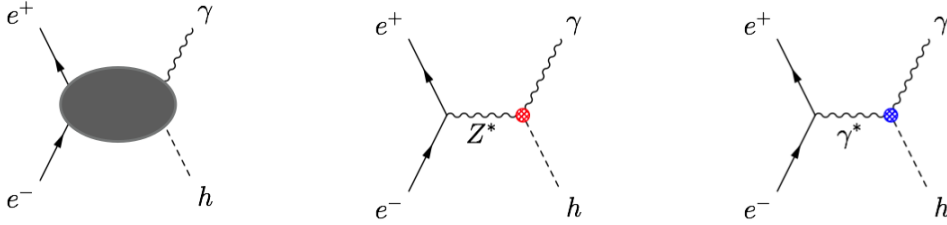


Figure 2: Diagrams arising from each of the three terms of Eq. 1, respectively.

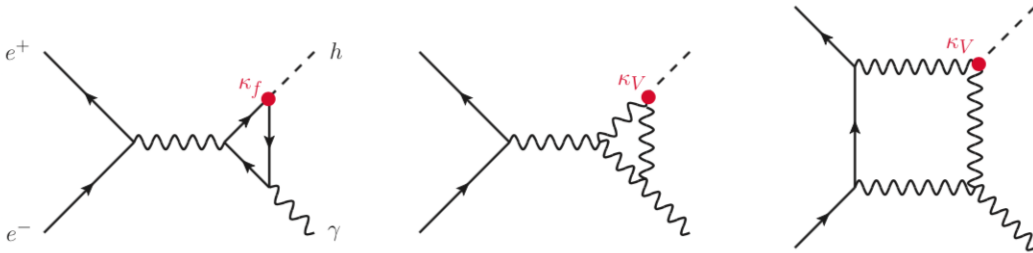


Figure 3: The loop induced Feynman diagrams in the Standard Model for $e^+e^- \rightarrow h\gamma$ [2]

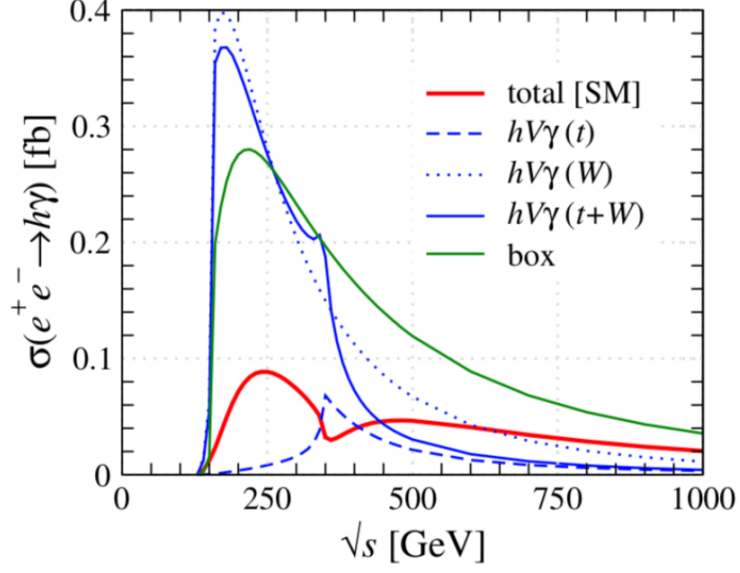


Figure 4: The contributions from individual diagrams of Fig. 3.

Table 1: SM cross sections for different beam polarizations ($\sqrt{s} = 250$ GeV).

P_{e^-}	P_{e^+}	$\sigma_{SM}[\text{fb}]$
-100%	+100%	0.35
+100%	-100%	0.016
-80%	+30%	0.20

3 Simulation Framework

We use fully-simulated Monte-Carlo (MC) samples produced with the ILD DBD model [6]. For event generators, we use PhysSim [7] for the signal, and Whizard [8] for background processes. We include all $e^+e^- \rightarrow 2$ -fermion (2f) and 4-fermion (4f) SM processes in the background. ISR and Beamstrahlung effects are included in the event generators. For detector simulation, we use Mokka [9], which is based on Geant4 [10], and for event reconstruction, we use Marlin in iLCSoft [11], where particle flow analysis (PFA) is done with PandoraPFA [12] and flavor tagging is done with LCFI+ [13]. The analysis is carried out at $\sqrt{s}=250$ GeV, assuming an integrated luminosity of 2 ab^{-1} with $P(e^-, e^+) = (-0.8, +0.3)$.

4 Combined Result

Previously, we reported an analysis of the $h \rightarrow b\bar{b}$ channel at LCWS2018 [14] that a signal significance of 0.53σ is expected for the SM cross section. Using this result and Eq. 5, we can set bounds on the parameter ζ_{AZ} ,

$$4.1 > \frac{\sigma_{\gamma H}}{\sigma_{SM}} = 1 - 201\zeta_A - 273\zeta_{AZ} > 0 \quad (4)$$

$$-0.011 < \zeta_{AZ} < 0.0037, \quad (5)$$

where $\zeta_A = 0$ is assumed and 4.1 is the 95% C.L. upper limit estimated with the simplified formula $1.64/\textit{significance} + 1$. We can set an additional bound in the same way using a previous study [4] which reported an expected significant of 2.31σ for the $h \rightarrow \gamma Z$ branching ratio.

$$1.71 > \frac{\text{BR}(h \rightarrow \gamma Z)}{\text{BR}_{SM}} = 1 + 290\zeta_{AZ} > 0 \quad (6)$$

$$-0.0034 < \zeta_{AZ} < 0.0024, \quad (7)$$

where 1.71 is the 95% C.L. upper limit. The expected combined 1σ bound on ζ_{AZ} is then

$$\frac{1}{\sigma_{\Delta\zeta}^2} = (290)^2(2.31)^2 + (-273)^2(0.53)^2 \quad (8)$$

$$-0.0015 < \zeta_{AZ} < 0.0015. \quad (9)$$

5 Fully Hadronic $h \rightarrow WW^*$ Decay Channel

5.1 Event Selection

The new signal channel study in this paper is $e^+e^- \rightarrow h\gamma$, followed by $h \rightarrow WW^*$, where both W s decay hadronically. In the final states of the signal events, we expect one isolated monochromatic photon with an energy of $E_\gamma = \sqrt{s}/2 \left(1 - (m_h/\sqrt{s})^2\right) = 93$ GeV, where m_h is the Higgs mass. The energy resolution of the electromagnetic calorimeter is typically

$\sigma_E = 0.16 \times \sqrt{E}$ (GeV), where the photon energy E is in units of GeV [6]. The energy resolution for the isolated photon is thus around 1.5 GeV. The main background we expect would be $e^+e^- \rightarrow W^+W^-$ with a hard ISR photon.

As pre-selection, we start with identifying one isolated photon with an energy greater than 50 GeV. Sometimes, the reconstruction software PandoraPFA splits calorimetric clusters created by a single high energy photon into several objects. Such split clusters fall within a narrow cone ($\cos\theta_{cone}=0.998$, where θ_{cone} is cone angle), and are combined into a single photon in the following analysis. The particles other than the photon are clustered into four jets using the Durham algorithm [15]. A pair of jets among the four jets, which has the invariant mass closest to $m_W = 80.4$ GeV, is combined to form the on-shell W , namely W_1 . And the other pair of jets is combined to form the off-shell W^* , namely W_2 . The four jets are combined to form the Higgs boson.

As the final selection, we first apply cuts to suppress 2-fermion background. We show the characteristics of signal and 2-fermion background in Table 2. We require the number of particles in each jet to be greater than 5, and the number of charged particles in each jet greater than 1. Then we demand $\log_{10}(y_{43}) > -2.5$ and $\log_{10}(y_{32}) > -1.8$, where y_{mn} is the jet distance parameter defined in the Durham jet-clustering at the step from m jets to n jets. In Fig. 5 the distributions of y_{32} and y_{43} are shown for the signal and background events.

Table 2: The characteristics for signal and 2-fermion background events

Signal	background	Effective cut
Many particles in a jet	few particles in jet ($e^+e^-/\mu^+\mu^-/\nu\bar{\nu}$)	# of particles in jet >5
Many charged particles in a jet	few charged particles in jet ($\tau^+\tau^-$)	# of charged particles in jet >1
large y_{43}, y_{32}	relatively small y_{43}, y_{32} ($q\bar{q}$)	y_{43}, y_{32}

We now try to suppress the 4-fermion background dominated by $e^+e^- \rightarrow W^+W^-(\gamma)$. Table 3 shows the characteristics for signal and background events. We apply the following cuts: $65 < m_{w1} < 90$, $20 < m_{w2} < 60$, $115 < m(4jets) < 135$, $90 < E_\gamma < 100$, where all the numbers are in units of GeV, and $|\cos\theta_\gamma| < 0.9$. The distributions of these variables are shown in Figs. 6, 7, 8.

Table 3: Characteristics of signal and 4-fermion background events.

Signal	background	Effective cut
one on-shell W	no W resonance (such as $ZZ \rightarrow 4f$)	W_1 mass
one off-shell W	two W resonances ($W^+W^- \rightarrow 4f$)	W_2 mass
h resonance	no h resonance	Higgs mass
monochromatic photon	Energy of photon small	γ energy
photon is not forward	photon is very forward	γ polar angle

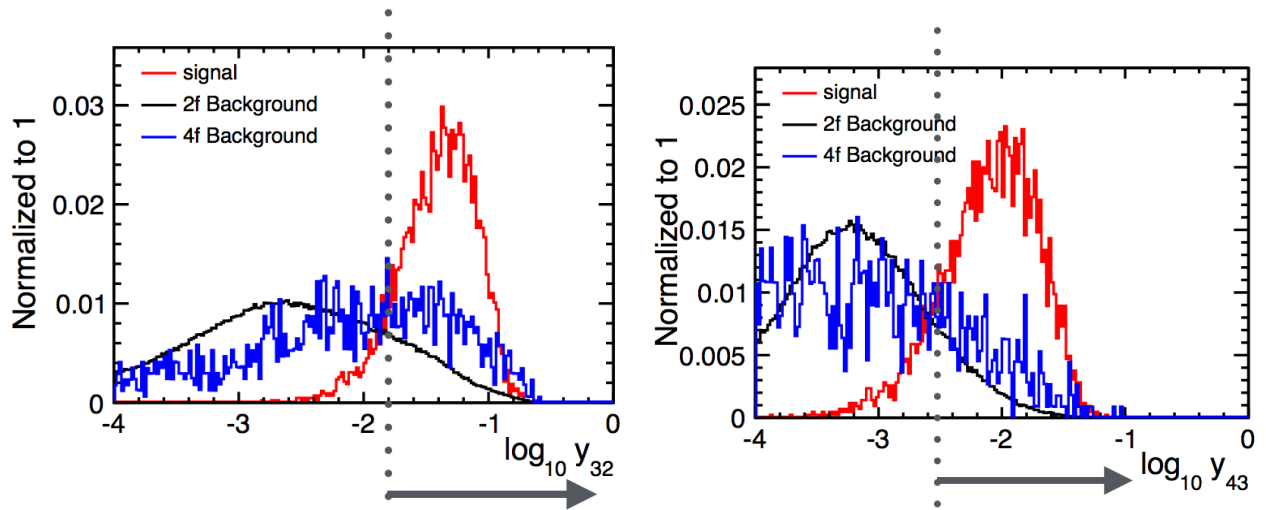


Figure 5: Distributions of y_{43} and y_{32} for signal and background events.

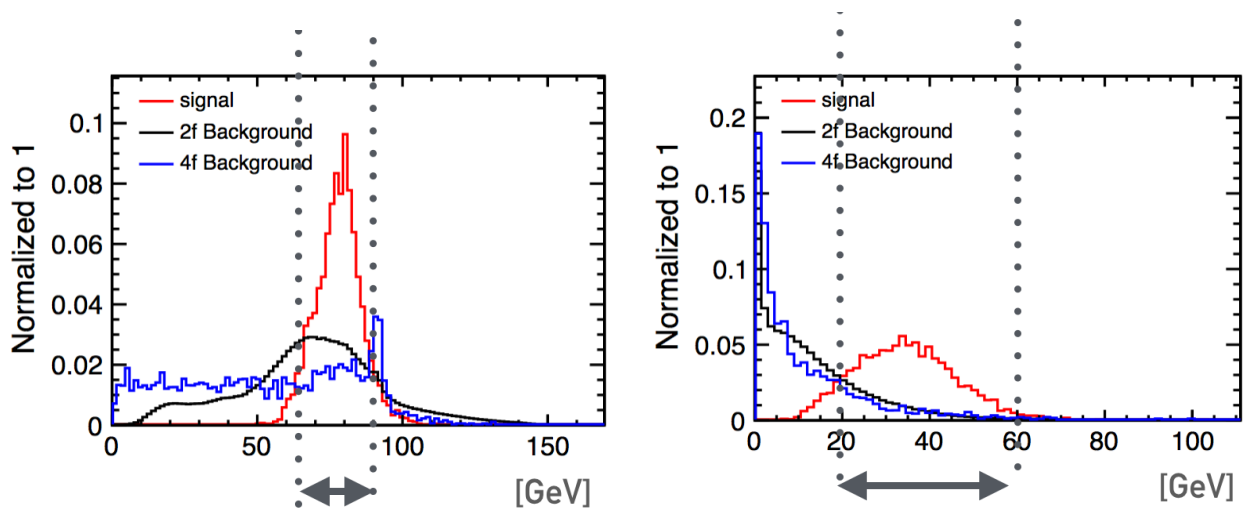


Figure 6: Distributions of m_{w1} (left) and m_{w2} (right) for signal and background events.

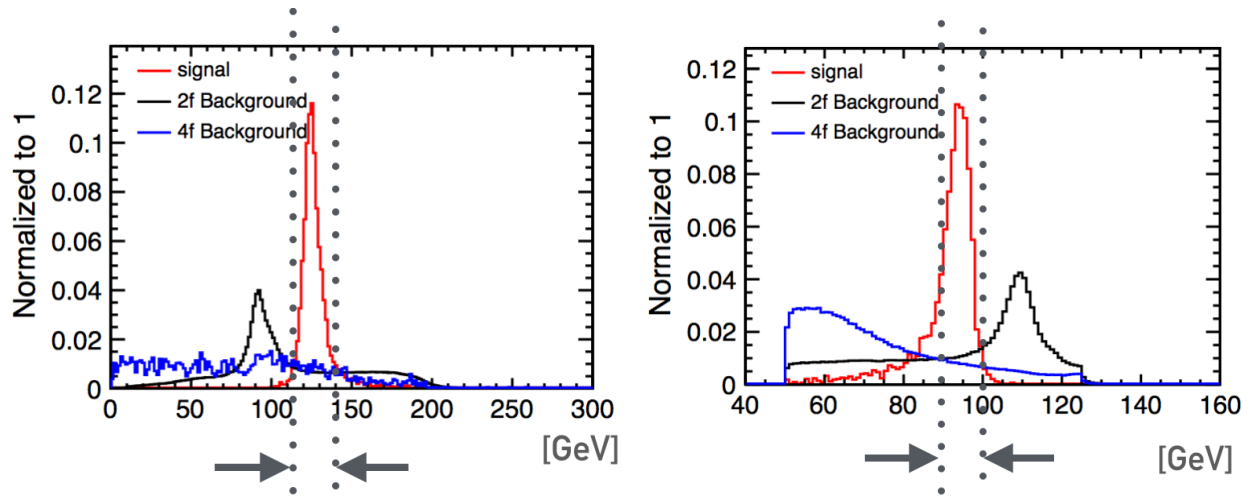


Figure 7: Distributions of reconstructed Higgs mass (left) and photon energy (right) for signal and background events.

As the final cut, we require the largest b -likeliness among the four jets (defined as $b_{\max 1}$) to be smaller than 0.7, to suppress events from $e^+e^- \rightarrow h\gamma$ followed by $h \rightarrow b\bar{b}$ and other background events (see Fig. 8).

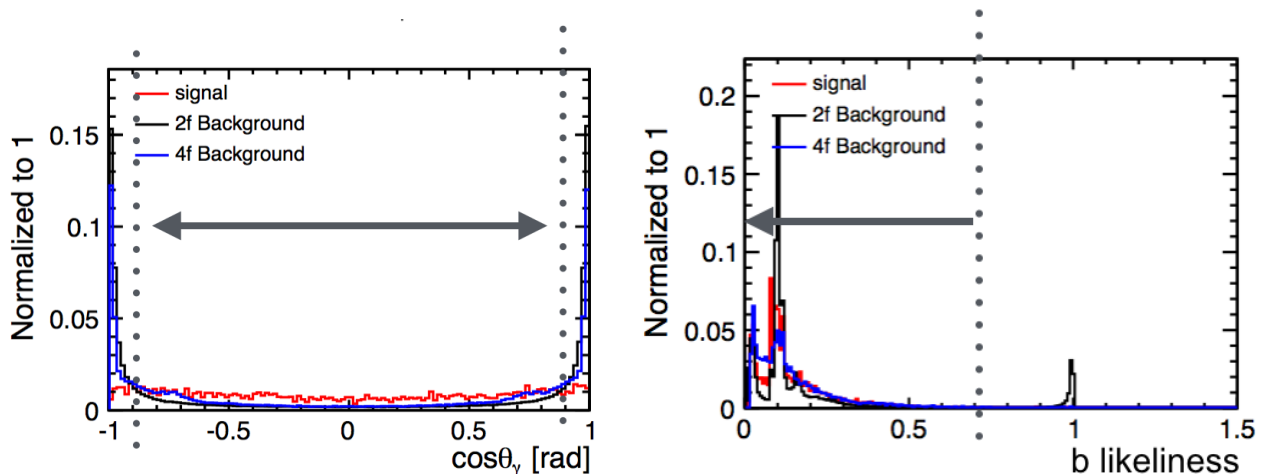


Figure 8: Distributions of cosine of photon polar angle (left) and the largest b -likeliness for signal and background events.

The cut values are optimized to maximize the signal significance defined as

$$\text{significance} = \frac{N_S}{\sqrt{N_S + N_B}}, \quad (10)$$

where N_S and N_B are the numbers of signal and background events, respectively.

5.2 Result

Table 4 gives the numbers of signal and background events, as well as the signal significance after each cut. The significance is defined by Eq. 10. After all the cuts, the signal significance is expected found to be 0.09σ , for the SM signal process $e^+e^- \rightarrow h\gamma$ followed by the fully hadronic $h \rightarrow WW^*$ decay.

6 Summary and Conclusions

In this paper, we have studied measurements of the $h\gamma Z$ coupling in two different ways, the first method is to measure the branching ratio of the $h \rightarrow \gamma Z$ decay and the other to measure the cross section for the $e^+e^- \rightarrow h\gamma$ process at the 250 GeV ILC, assuming 2 ab^{-1} data collected by the International Large Detector (ILD). We found the expected 1σ bound on the effective $h\gamma Z$ coupling (ζ_{AZ}): $-0.0015 < \zeta_{AZ} < 0.0015$, combining measurements of the cross section for $e^+e^- \rightarrow h\gamma$ followed by $h \rightarrow b\bar{b}$ and the $h \rightarrow \gamma Z$ branching ratio. We have also performed a full simulation for the fully hadronic $h \rightarrow WW^*$ channel and found the expected signal significance of 0.09σ for beam polarizations of $P(e^-, e^+) = (-80\%, +30\%)$.

Table 4: Reduction table for the signal and background events after each cut

	Signal	background	Significance
Expected	40.2	3.14×10^8	0.005
Pre selection	37.7	6.10×10^7	0.01
# of particle >5	32.0	1.12×10^7	0.01
# of charged particle >1	25.9	6.65×10^6	0.01
$\log 10(y_{43}) > -2.5$			
$\log 10(y_{32}) > -1.8$	20.9	1.52×10^6	0.02
$65 < m_{w1} < 90$	18.9	8.60×10^5	0.02
$20 < m_{w2} < 60$	17.4	5.59×10^5	0.02
$115 < m(4jets) < 135$	15.7	7.44×10^4	0.06
$90 < E_\gamma < 100$	11.8	2.73×10^4	0.07
$-0.9 < \cos\theta < 0.9$	10.3	1.45×10^4	0.09
b likliness < 0.7	10.0	1.36×10^4	0.09

We are planning to improve our analysis by adding the $h \rightarrow WW^*$ semi-leptonic channel. After the analysis of $h \rightarrow WW^*$ channel is completed, we will combine the bounds on ζ_{AZ} from different channels, and translate the combined bound into that on Dimension-6 operators. We will then investigate the role of the combined bound in one global EFT analysis.

Acknowledgements

We would like to thank the LCC generator working group and the ILD software working group for providing the simulation and reconstruction tools and producing the Monte Carlo samples used in this study. This work has benefited from computing services provided by the ILC Virtual Organization, supported by the national resource providers of the EGI Federation and the Open Science GRID.

References

- [1] T. Behnke *et al.*, “The International Linear Collider Technical Design Report - Volume 1: Executive Summary,” arXiv:1306.6327 [physics.acc-ph].
- [2] S. Kanemura, K. Mawatari and K. Sakurai, “Single Higgs production in association with a photon at electron-positron colliders in extended Higgs models,” arXiv:1808.10268 [hep-ph].
- [3] Cepeda, M. and others, “Report from Working Group 2’,” CERN Yellow Rep. Monogr 7 ,2019 221-584. arXiv:1902.00134[hep-ph]
- [4] K. Fujii, Y. Kato, J. Tian, S. Yamashita, “Study of HZ branching ratio at the ILC 250GeV,” LCWS2018.
- [5] Junping Tian, Keisuke Fujii, and Hiroshi Yokoya, “Diphoton resonances at the ILC” Phys.Rev. D94 (2016) 095015.
- [6] T. Behnke *et al.*, “The International Linear Collider Technical Design Report - Volume 4: Detectors,” arXiv:1306.6329 [physics.ins-det].
- [7] Physsim home page <http://www-jlc.kek.jp/subg/offl/physsim/>
- [8] W. Kilian, T. Ohl and J. Reuter, “WHIZARD: Simulating Multi-Particle Processes at LHC and ILC,” Eur. Phys. J. C **71**, 1742 (2011) doi:10.1140/epjc/s10052-011-1742-y [arXiv:0708.4233 [hep-ph]].
- [9] Mokka Home page, http://ilcsoft.desy.de/portal/software_packages/mokka/
- [10] S. Agostinelli et al. (GEANT4 Collaboration), “Geant4a simulation toolkit,” Nucl.Instrum. Methods Phys. Res., Sect. A **506**, 250 (2003).
- [11] F. Gaede, J. Engels, “Marlin et al - A Software Framework for ILC detector R&D,” EUDET-Report-2007-11.
- [12] M. A. Thomson, “Particle Flow Calorimetry and the PandoraPFA Algorithm,” Nucl. Instrum. Meth. A **611**, 25 (2009) doi:10.1016/j.nima.2009.09.009 [arXiv:0907.3577 [physics.ins-det]].
- [13] T. Suehara and T. Tanabe, “LCFIPlus: A Framework for Jet Analysis in Linear Collider Studies,” Nucl. Instrum. Meth. A **808**, 109 (2016) doi:10.1016/j.nima.2015.11.054 [arXiv:1506.08371 [physics.ins-det]].
- [14] Y Aoki, K Fujii, S Jung, J Lee, J Tian, H Yokoya, “Study of $H \rightarrow Z\gamma$ branching ratio at the ILC 250GeV,” arXiv:1902.06029.
- [15] S. Catani, Y. L. Dokshitzer, M. Olsson, G. Turnock and B. R. Webber, “New clustering algorithm for multi - jet cross-sections in e+ e- annihilation,” Phys. Lett. B **269**, 432 (1991). doi:10.1016/0370-2693(91)90196-W